International Journal for Housing Science and Its Applications
Publish August 6, 2025. Volume 46, Issue 3 Pages 6159-6170

https://doi.org/10.70517/ijhsa463529

Study on microscopic heat conduction mechanism of metallurgical materials based on lattice Boltzmann approach

Hongye He[1], Shubao Wang[1,*], Junli Yu[1] and Wenhui Liu[1]
[1] Qian'an College, North China University of Science and Technology, Qian'an, Hebei, 064400, China
Corresponding authors: (e-mail: 18232566700@163.com).

Abstract The microscopic heat transfer mechanism of metallurgical materials has a significant impact on the material properties, and the traditional numerical methods are difficult to deal with complex boundary conditions and multi-scale heat transfer problems. In this paper, the lattice Boltzmann method (LBM) is adopted to study the microscopic heat transfer mechanism of metallurgical materials, and a large-vortex simulation framework based on the D3Q19 model is established, and the coupling of the phase field method and the lattice Boltzmann method (PF-LBM) is realized. The study simplifies the Boltzmann equation through the BGK collision operator, introduces the Smagorinsky sublattice model to deal with turbulence, and employs the bounce format and the nonequilibrium extrapolation format to deal with boundary conditions. The flow field, temperature field, solute field and phase field are coupled to realize the multi-field coupled simulation in micro-macroscopic scale. The results show that in the simulation of heat transfer power loss of the torque converter, the simulated value of 15.62 kW agrees well with the experimental value of 16.82 kW when the rotational speed is 1600 r/min; in the simulation of discontinuous heat transfer in nanoscale, the D2Q37 lattice model effectively overcomes the internal unphysical temperature jump effect and the boundary accuracy is improved by 27% when Kn = 0.42. The conclusion confirms that the method can accurately simulate the heat transfer process of metallurgical materials at different scales, which provides a theoretical basis for optimizing the thermal properties of materials.

Index Terms Lattice Boltzmann method, Microscopic heat transfer, Large-vortex simulation, Phase-field method, Multi-field coupling, Nanoscale

I. Introduction

Mesoscopic kinematics methods based on the Boltzmann equation have been the hotspot and frontier of computational fluid dynamics research in recent years, and nowadays a variety of algorithms, such as the lattice Boltzmann method (LBM), gas kinematics format (GKS), gas kinematics algorithm (GKFS), and the lattice Boltzmann flux algorithm (LBFS), have been developed [1]-[4]. This class of algorithms not only effectively connects the macroscopic computational fluid dynamics methods oriented to continuous media and the microscopic computational methods based on molecular kinetics, but also has been successfully applied in many complex flows of metallurgical materials [5].

The lattice Boltzmann algorithm has been continuously developed in recent years and has now been applied to a number of fields such as moving boundaries, multiphase flows, incompressible isothermal flows, incompressible heat transfer fluid flows and incompressible conjugate heat transfer problems [6]. For example, Liu, Y et al [7] used the lattice Boltzmann method to simulate non-Fourier heat transfer and analyzed the effects of relaxation time, shape, and substrate temperature oscillations on heat transfer efficiency under periodic boundary conditions. Kiani-Oshtorjani, M et al [8] used a novel lattice Boltzmann method to investigate the conjugate heat transfer phenomenon in mixtures of fluids and particle clusters and also explored its effect on thermal conductivity based on the particle contact and thermal conductivity ratio. Mishra, S. C et al [9] extended the lattice Boltzmann method to the study of radiative heat transfer mechanisms in one-dimensional planar media by introducing a new lattice for volumetric radiative calculations and verifying the accuracy of the results by using it with the finite volume method. Samian, R. S et al [10] used a finite volume lattice Boltzmann method to simulate transient heat transfer from the macroscopic scale to the microscopic nanoscale, validating the model against Fourier's law.

It is important to note that flow and heat transfer in the field of metallurgical materials often occur in complex regions or within porous media [11]. These two types of problems involve complex heat-flow-solid interactions, thus designing efficient algorithms for these two types of problems is a challenging task [12]. Traditional numerical methods use finite difference and finite element methods to obtain detailed information about the flow field as well as the temperature field, etc. The LBM method has many advantages that are unmatched by the traditional methods,

and is well suited for dealing with flow and heat transfer problems under complex boundaries and in porous media [13], [14]. Qin, X et al [15] used the lattice Boltzmann method and fractal model to simulate and analyze the heat transfer mechanism in porous media and explored its effectiveness in predicting thermal conductivity and understanding the thermophysical mechanisms. Wang, C. H et al [16] also used the lattice Boltzmann method to numerically simulate the convective heat transfer mechanism in a porous medium with a rectangular heat source and explored the effects of various parameters on the heat exchange and flow field, and validated the results by comparing them with experimental data. Abchouyeh, M. A et al [17] numerically investigated water based nanofluid containing Cu nanoparticles, flowing in a channel and natural convection heat transfer by using lattice Boltzmann method and analyzed the effect of different parameters on the heat transfer efficiency.

The heat transfer characteristics of metallurgical materials directly affect their processing and utilization properties, while the micro-scale heat transfer mechanism is the fundamental factor determining the macroscopic thermal properties of materials. The traditional continuum mechanics approach has limitations in dealing with the microscale heat transfer problem, especially in the case of significant interfacial effects and scale effects, the accuracy of the classical heat transfer theory decreases dramatically. The lattice Boltzmann method, as a mesoscopic numerical method based on molecular dynamics theory, describes the fluid flow and heat transfer process by tracking the evolution of the distribution function of discrete particles, and shows unique advantages in dealing with the problems of complex boundaries, multiphase flow, and micro- and nanoscale heat transfer. The method is not only able to naturally deal with complex geometries and boundary conditions, but also able to reveal the physical mechanism of heat transfer directly from the microscopic level. In recent years, the application of the lattice Boltzmann method in the field of materials science has gradually increased, especially in the study of heat and mass transfer during the solidification process of materials, phase transition dynamics, etc. Important progress has been made. However, combining the lattice Boltzmann method with other numerical methods to construct a computational framework for multi-scale and multi-physics field coupling is still a challenging research topic. In this study, a numerical simulation framework for microscopic heat transfer in metallurgical materials is constructed based on the lattice Boltzmann method, which employs the D3Q19 lattice model and the BGK collision operator, and combines with the large eddy simulation technique to deal with turbulence effects. By coupling the lattice Boltzmann method with the phase field method, a multi-field coupling model of PF-LBM is established to realize the synergistic evolution of the flow field, temperature field, solute field and phase field. The research focuses on solving the key technical problems such as boundary condition processing, parameter dimensionlessness and data exchange between multi-fields. The accuracy and applicability of the established model are verified through two typical cases, namely, the simulation of heat conduction power loss in torque converter and the simulation of discontinuous heat transfer at nanoscale, to reveal the heat conduction mechanism of metallurgical materials at different scales.

II. LBM-based simulation model of microscopic heat transfer in metallurgical materials

II. A. Lattice Boltzmann Method (LBM)

The lattice Boltzmann method (LBM) [18], as a numerical simulation method for complex flows, has the advantages of simple form and easy handling of complex boundaries, and has received extensive attention from scholars.

In the LBM method, a simple regular distribution function of microscopic particles is used to represent the discrete particles in a certain velocity space and position space, and the discrete particles are bound to the corresponding grid nodes, and the discrete velocity model is established through the evolution equation to derive the distribution function of discrete particles, and then the macroscopic variables, such as density and velocity, are obtained by the direct calculation based on the distribution function of the particles.The LBM calculates the macroscopic density of the fluid based on the distribution function and macroscopic velocity, which is different from the traditional numerical method of directly discretizing and solving the Navier-Stokes equations, and its derivation process is similar to the molecular dynamics model (MD).

Boltzmann equation is based on the systematic theory, combined with microscopic discrete particles and macroscopic fluid flow through the mesoscopic method for describing the non-equilibrium state of the distribution function evolution law of the equation, can also be obtained from the continuous Boltzmann equation. the basic model of the LBM is currently D1Q3, D2Q5, D2Q9, D3Q19 and so on.

The Boltzmann equation is a conservation equation that describes the spatial and temporal variation of the particle velocity distribution function f:

$$\frac{\partial f}{\partial t} + \xi \cdot \nabla f = \Omega(f) \tag{1}$$

where ξ denotes the velocity of the particle and $\Omega(f)$ is the collision operator that represents the effect of the collision. Discretization of this equation yields the lattice Boltzmann equation (LBE):

$$f_i(x+c_i\Delta t,t+\Delta t)-f_i(x,t)=\Omega_i(f) \tag{2}$$

Due to the extremely complex nonlinear integrals of the collision operator design, the Boltzmann equation is very limited in its application, and many kinds of simplified collision operators or collision models have been proposed for this purpose.The BGK model is the simplest and the most commonly used collision operator model, which is represented by the collision operator as:

$$\Omega_i=-\frac{1}{\tau}\left[f_i(x,t)-f_i^{eq}(x,t)\right] \tag{3}$$

With the introduction of the BGK model, the lattice Boltzmann equation can be approximated as:

$$f_i\left(x+c_i\Delta t,t+\Delta t\right)-f_i(x,t)=-\frac{1}{\tau}\left[f_i(x,t)-f_i^{eq}(x,t)\right] \tag{4}$$

where $f_i(x,t)$ is the distribution function of the discrete velocity of the particle at moment x at moment t for c_i, τ is the relaxation time, Δt is the time step, and f_i^{eq} is the corresponding equilibrium state distribution function.

Among the BGK models, the $DnQb$ model (n is the number of spatial dimensions and b is the number of discrete velocities) is the most representative.The D3Q19 model has 19 discrete velocities in three dimensions.

In the D3Q19 model, the equilibrium distribution function can be expressed as:

$$f_i^{eq}(x,t)=\omega_i\rho\left[1+\frac{c_i\cdot u}{c_s^2}+\frac{(c_i\cdot u)^2}{2c_s^4}-\frac{u^2}{2c_s^2}\right] \tag{5}$$

where ω_i is the weighting factor and c_s is the speed of sound.

$$c_s=\frac{c}{\sqrt{3}},\quad \omega_i=\begin{cases}1/3, & c_i^2=0\\ 1/18, & c_i^2=c^2\\ 1/36, & c_i^2=2c^2\end{cases} \tag{6}$$

The macroscopic density and macroscopic velocity can be calculated from equation (7):

$$\rho=\sum_i f_i,\rho u=\sum_i c_i f_i \tag{7}$$

II. B. Large eddy simulation based on the lattice Boltzmann method

The Large Eddy Simulation (LES) [19] method is a spatial averaging of turbulent pulsations that separates large-scale eddies from small-scale eddies by some filter function, where large-scale eddies are simulated directly and small-scale eddies are closed by a model. The basic approach to large eddy simulation is to simulate large-scale motions by directly solving the N-S equations and small-scale motions by sublattice format. The first step in large eddy simulation is to perform a filtering operation:

$$\overline{w}(x)=\int w(x)G(x,x')\mathrm{d}x' \tag{8}$$

where w is the velocity, density and other flow field macroscopic quantities, and G is the spatial filtering function. Assuming that the filtering process and the derivation process can be exchanged and the filtering operation is used in the N-S equation, the corresponding filtering control equation can be obtained.

Continuity equation:

$$\frac{\partial\overline{u}_i}{\partial x_i}=0 \tag{9}$$

Momentum equation:

$$\frac{\partial\overline{u}_i}{\partial t}+\overline{u}_j\frac{\partial\overline{u}_i}{\partial x_j}=-\frac{1}{\rho}\frac{\partial\overline{p}}{\partial x_j}-\frac{\partial\tau_{ij}}{\partial x_j}+\frac{\partial}{\partial x_j}\left[\nu\left(\frac{\partial\overline{u}_i}{\partial x_j}+\frac{\partial\overline{u}_j}{\partial x_i}\right)\right] \tag{10}$$

where τ_{ij} is the Reynolds stress: $\tau_{ij}=\overline{u_iu_j}-\overline{u}_i\overline{u}_j$.

Currently, the more commonly used subgrid-scale model for turbulence is the Smagorinsky model:

$$\tau_{ij}-\frac{\delta_{ij}}{3}\tau_{kk}=C\Delta^2\left|\overline{S}\right|\overline{S}_{ij}=\nu_t\overline{S}_{ij} \tag{11}$$

$$\left|\overline{S}\right|=\sqrt{2\overline{S}_{ij}\overline{S}_{ij}} \tag{12}$$

$$\overline{S}_{ij}=\frac{1}{2}\left(\frac{\partial\overline{u}_i}{\partial\overline{x}_j}+\frac{\partial\overline{u}_j}{\partial\overline{x}_i}\right) \tag{13}$$

where δ_{ij} is the Kronecker tensor; ν_t is the vortex viscosity coefficient; $|\overline{S}|$ is the mode of the large-scale strain tensor $\overline{S}_{ij}$; C is Smagorinsky's constant, $C>0$; and Δ is the filter width.

In this paper, we use large eddy simulation (LBM-LES) based on the lattice Boltzmann method, following the idea of the Smagorinsky sublattice model [20], keeping the equilibrium distribution function in the model unchanged, as well as the relation between the chirp time and the viscosity in the original model, viz:

$$\nu_{tot}=\frac{2\tau_{tot}-1}{6} \tag{14}$$

In Eq. (15), the total viscosity coefficient ν_{tot} is divided into two components, the physico-dynamic viscosity ν_0 and the eddy viscosity ν_t:

$$\nu_{tot}=\nu_0+\nu_t \tag{15}$$

Eq. $\nu_t=C\Delta^2\left|\overline{S}\right|$.

thus obtaining:

$$\tau_{tot}=3\nu_{tot}+\frac{1}{2}=3\left(\nu_0+C\Delta^2\left|\overline{S}\right|\right)+\frac{1}{2} \tag{16}$$

Derived from the unbalanced part of the distribution function of the filtered nodes:

$$\left|\overline{S}\right|=\frac{\sqrt{\nu_0^2+18C\Delta^2Q^{1/2}}-\nu_0}{6C\Delta^2} \tag{17}$$

$$Q^{1/2}=\left(\tau_0+3C\Delta^2\left|\overline{S}\right|\right)\frac{2n}{3}\left|\overline{S}\right| \tag{18}$$

$$\tau_0=3\nu_0+\frac{1}{2} \tag{19}$$

By joining the above equations, $\left|\overline{S}\right|$ can be obtained.

At this point, the evolution equation for D3Q19 becomes:

$$\overline{f}_i(x+c_i\Delta t,t+\Delta t)-\overline{f}_i(x,t)=-\frac{1}{\tau_{tot}}\left[\overline{f}_i(x,t)-\overline{f}_i^{eq}(x,t)\right] \tag{20}$$

The total collision operator in the BGK model can be solved by bringing in τ_{tot}, $|\overline{S}|$, and substituting into the evolution equation.

II. C. Computational parameters and boundary conditions

The geometry of the computational domain for the numerical simulation of the backstage flow is shown in Fig. 1. The fluid flows along the X-axis from the left side of the channel with the velocity calculated from the Reynolds number, which is changed by changing the inlet velocity, and exits from the right side of the channel at the outlet, which is a pressure outlet with a pressure of 101 kPa. The upper and lower walls and the step wall are in the standard rebound format while the front and rear walls of the channel are in the non-equilibrium extrapolated boundary conditions. The step is located on the left side of the channel and has a length of L, a width of D and a height of H. The length of the channel is L_c, the width is D_c and the height is H_c.

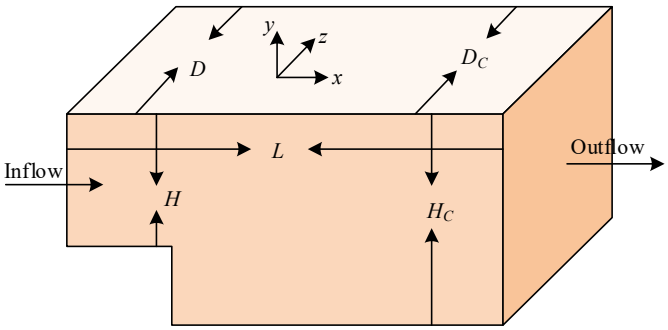

Figure 1: The three-dimension al model of back- facing step flow

Boundary Condition Processing When using some kind of macroscopic physical boundary conditions to process the boundary problem in the lattice Boltzmann method, the appropriate boundary format will have a direct impact on the numerical accuracy, stability and solution efficiency. In the LBM model, the macroscopic physical quantities are not involved in the evolution, and the distribution function of the internal flow field nodes can be obtained by using the collision and migration rules, and the part of the distribution function on the boundary nodes has to be determined according to the known boundary condition settings or macroscopic physical quantities. Choosing a reasonable boundary processing method can improve the numerical computation accuracy, computational efficiency and computational stability. In this paper, the solid-liquid boundary of the flow field is processed using the bounce format, the external boundary of the solute field is used as a diffusion-free boundary, the solid-liquid boundary is used in the bounce format, and the temperature field does not deal with the solid-liquid boundary, and the external boundary is used in the non-equilibrium extrapolation format.

(1) Bounce format

Bounce format is a simulation of stationary solids, the most commonly used processing method to deal with moving boundary conditions. Along the solid wall of the boundary movement of the incident particles touch the solid wall, to the opposite direction of the movement of the rebound back to the fluid domain, before and after the collision of the speed of the moving particles does not change, but the direction of movement is opposite. This rebound format is easy to implement, easy to write the program, can ensure that the system's mass, momentum conservation and no slip velocity, the solution accuracy is only first order.

(2) Non-equilibrium extrapolation format

The basic idea of the non-equilibrium extrapolation format is to decompose the distribution function on the boundary into two parts: the equilibrium distribution function that constructs a new approximate equilibrium state according to specific macroscopic boundary conditions and the non-equilibrium distribution function that uses the non-equilibrium portion of the adjacent fluid node to replace the non-equilibrium distribution function, and the non-equilibrium distribution function is determined by extrapolation using the first-order accuracy. The format has second-order accuracy and can well handle flow boundary problems such as velocity and pressure boundaries, and can also be used to deal with isothermal and adiabatic boundary problems for thermal flows.

II. D. PF-LBM coupling modeling

The phase field method (PFM), as the most effective method to simulate the phase transition process of alloy solidification microstructure evolution, introduces the phase field variables in the phase field control equation, and couples the LBM flow field and external fields such as the temperature field and solute field into the phase field, realizing the multifield coupled phase field model on the micro-macro scale. The key to the multi-field coupled phase field model is how to reasonably and effectively combine the lattice Boltzmann method for calculating the flow field and the phase field method.

In the multi-field coupled phase-field simulation, the effect produced by heat and solute will change the original symmetric growth morphology of dendrites. Therefore, in each time step calculation process, it is necessary to calculate the phase field temperature value, solute concentration value and phase field value of the next time step based on the current time step, and recalculate the velocity value u and velocity distribution function of the flow field in different spatial nodes using the LBM method. The relaxation steps of the concentration and temperature particle distribution functions are then calculated by substituting the different time-states flow velocity values u into the new round of equilibrium particle distribution function equations for the temperature and solute fields. The phase field, solute field, temperature field and flow field interact with each other and produce effects on each other to simulate the growth morphology state of dendrites under the effect of flow field. Based on the aforementioned set of equations

describing the phenomenon of diffusive convection, natural convection in the solidification field can be simulated at the same time. This chapter describes the establishment of the multi-field coupled phase field model and the process of realizing the PF-LBM model.

In this paper, the Fortran language is used to write the program for the control equations and calculation methods, and visualstudio software is used to carry out evolutionary calculations to simulate and reproduce the evolution of the microstructure of dendrites during the solidification process of nickel-based high-temperature alloys, and to compare and analyze the process of dendrites growth in forced and natural convection environments, as well as dendrites moving and growing. The program is mainly composed of three parts: pre-processing, computational simulation and post-processing, and the overall program calculation flow is shown in Figure 2.

The specific calculation steps are:

(1) Set parameters, such as interface thickness, discrete velocity, weighting factor, etc., and set the initial conditions and boundary conditions of temperature field, solute concentration field and flow field.

(2) Calculate the phase field distribution in the simulation region at the current moment with the phase field model and update the position of the dendrite to complete the phase field migration.

(3) Calculate the melt flow velocity u at each point in the simulation region at the current moment using the LBM model, simulate the growth of dendrites under convection only without movement when the solid is regarded as a stationary obstacle and the velocity within the solid is always 0. To simulate the movement of the dendrites need to calculate the external force applied to the solid, the dendrites' density and mass, and to calculate the solid's movement velocity u_S .

(4) Bring the melt flow velocity calculated in step (3) to solve the solute concentration distribution and realize the effect of flow velocity on solute transport.

(5) Store the data. The phase field variables, solute concentration and flow field at each point in the simulation process are stored in an array, and the data in the array are output to a numerical file of a specific format at certain time steps during the calculation process.

(6) Repeat steps (2)-(5) until the end conditions are met.

(7) Data post-processing. Using Tecplot360 mapping software to read the data file to achieve the visualization of the simulation results, so as to be able to more intuitively observe the microstructure morphology, concentration distribution, flow field distribution of the variable changes, as well as other physical quantities required for analysis.

Through the above steps, the calculation of the flow field distribution and the coupling between the dendrite growth and motion processes are completed. Therefore, the present model is able to reproduce the three-transfer process during the solidification of binary alloys and simulate and analyze the influence mechanism of melt flow on dendrite growth and motion.

II. E. Model Physical Properties and Calculation Parameters

The determination of the parameters for the numerical simulation of the phase-field method includes the determination of the interfacial thickness, the kinetic parameters of the phase field, and the spatial and temporal step sizes.

The gradient term coefficients $\varepsilon_{SS}(\varepsilon_{SL})$ and the height of the double-well potential $\omega_{SS}(\omega_{SL})$ are jointly determined by the interfacial energy σ and the interfacial thickness 2ξ of the solid-liquid or solid-solid interface:

$$\varepsilon_{SL}=\frac{4}{\pi}\sqrt{\xi_{SL}\sigma_{SL}};\quad w_{SL}=\frac{2\sigma_{SL}}{\xi_{SL}} \tag{21}$$

$$\varepsilon_{SS}=\frac{4}{\pi}\sqrt{\xi_{SS}\sigma_{SS}};\quad w_{SS}=\frac{2\sigma_{SS}}{\xi_{SS}} \tag{22}$$

Adjusting different ratios of σ_{SL} and σ_{SS} can change the wettability of the interface, and in this paper we set $\sigma_{SS}=2.5\sigma_{SL}$. $\xi_{SL}=\xi_{SS}$ to ensure that the grain boundaries can be wetted by the liquid phase under equilibrium conditions. Due to the small growth rate of dendrites, the interfacial kinetic coefficients are neglected, and the kinetic coefficients of the phase field at the solid-liquid interface are obtained as:

$$M_{SL}=\frac{8V_m\sigma_{SL}D_L\sqrt{2w_{SL}}}{\pi RT(1-k)^2c_e^*\varepsilon_{SL}^3} \tag{23}$$

Since the grid size and time step not only determine the computational parameters of the interpolation algorithm, but also affect the accuracy of the phase field model solution. Due to the great temperature gradient and cooling rate in the molten pool, a smaller grid size and time step are needed to ensure the convergence of the phase field calculation results, but the more the number of grids in the whole system, the larger the computational volume. Set

$dx = dy = 1\mu m$, the thickness of solid-liquid interface and solid-solid interface are set to $5 * dx$, the average radius of the initial nucleus is set to $3 * dx$, the pumping speed is set to $300\mu m / s$ for simulating the growth of directionally solidified columnar crystals, and the time step dt should be satisfied:

$$dt_1 \le \frac{(dx)^2}{5M_s\varepsilon^2} \tag{24}$$

$$dt_2 \le \frac{(dx)^2}{5D_L} \tag{25}$$

To ensure the accuracy and stability of the calculation results, the smaller of dt_1 and dt_2 is selected for the time step in the actual calculation process.

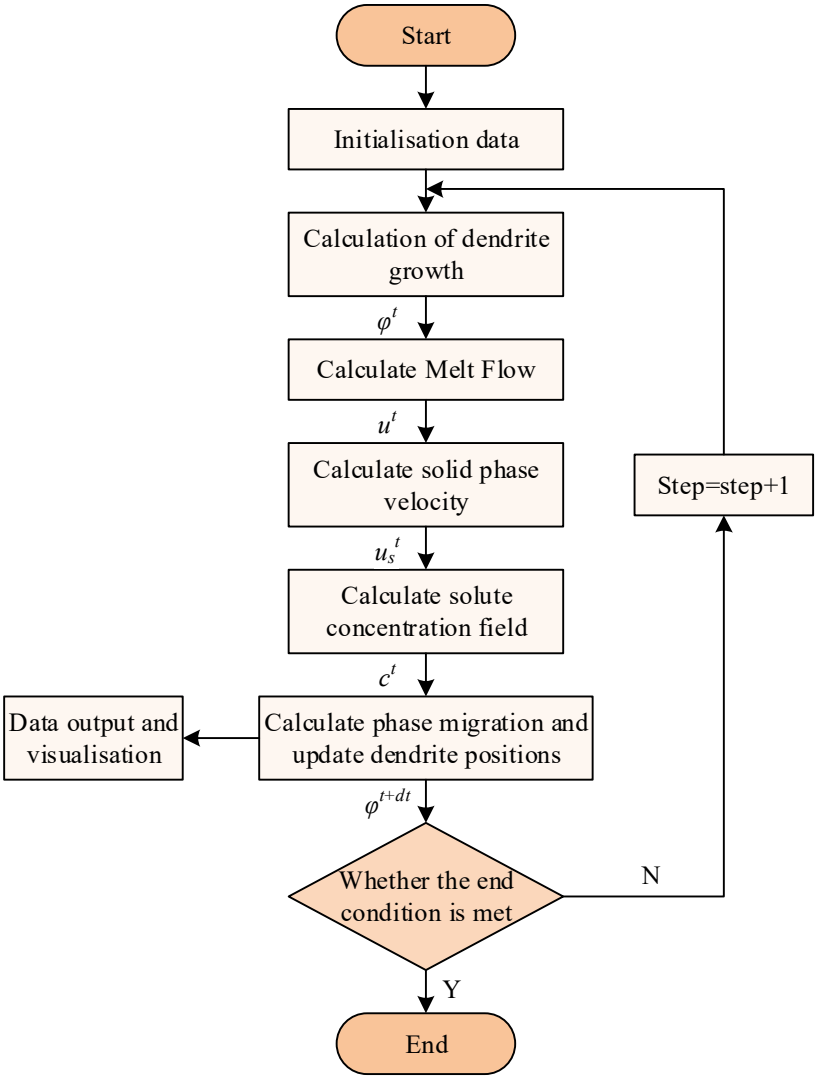

Figure 2: Overall program calculation flow chart

When model coupling is carried out, the parameters used need to be dimensionless, and the length, time and velocity are normalized with the lattice size Δx, time increment Δt and velocity $\Delta x / \Delta t$, respectively, and linked to the real physical parameters to reflect the real solidification process. The dimensionless length is obtained from the ratio of the real physical length and the length conversion factor, so that the dimensionless time unit and the unit length are 1. The velocity and acceleration conversion factors are calculated, and then the parameters such as the

solute diffusion coefficient, the melt flow velocity, and the gravitational acceleration are obtained after dimensionlessness. There are two important parameters in describing the fluid flow as Rayleigh number $\left(Re=\frac{uh}{\nu}\right)$ and smithsonian number $\left(Sc=\frac{\nu}{Dl}\right)$, which are the ratio of velocity and viscosity and the ratio of viscosity and diffusion coefficient, respectively, so the Rayleigh number Re and smithsonian number Sc are kept unchanged in the parameter dimensionless treatment. The melt viscosity coefficient is reduced to 1/82 of the original due to the limiting nature of the lattice Boltzmann.

In order to keep the dendrite tip always inside the calculation region when simulating the growth of directionally solidified columnar crystals, the program is set to initially grow the dendrite upward in the nucleus at the bottom of the calculation region, and when the dendrite grows to the point that the number of lattices between the tip and the upper boundary is less than 1/2 of the height of the whole simulation region, then it starts to execute the successive pull-out lattice method. That is, every time the tip of the dendrite passes through a grid, the height of the lower boundary is drawn one grid, while the upper boundary is replenished with the liquid phase with initial concentration and initial flow rate until the end condition of the calculation is reached. Such a treatment not only saves simulation time and improves the computational efficiency to a certain extent, but also ensures that the stable growth of dendrites is not affected by the upper boundary of the computational region.

III. Simulation test verification

III. A. Heat transfer power loss simulation test

The simulation model of heat conduction power loss of the torque converter limits the axial distance of the rotating parts to 15 mm, and the minimum radial distance to 25 mm.The experimental values of heat conduction power loss of the torque converter under the design working conditions are shown in Table 1. When the operating temperatures are 48° C and 55° C, the lubricant density is about 820 kg / m^3 and the dynamic viscosity is 0.055 Pa • s. In the simulation process carried out by the XFlow software, the particle tracking method and the large vortex simulation are used for the calculations, and the boundaries are processed by the Auto-matic method. The simulation time step is 0.0005 s, and the lattice resolution scale is 2.6 mm. A multiphase flow model is used, i.e., the heat transfer power loss described in the paper is the joint action of air and oil.

Table 1: Comparison of heat transmission loss simulation results

Test condition			Heat transmission loss/kW	
Liquid level/mm	Temperature/℃	Speed (r/min)	Test value	Simulation value
240	48	1000	5.74	4.88
		1200	8.61	8.69
		1400	11.91	11.93
		1600	16.82	15.62
		1800	20.24	22.15
		2000	23.92	27.45
		2200	29.36	42.95
280	52	1000	6.25	5.47
		1200	9.22	8.59
		1400	12.35	12.59
		1600	16.84	20.04
		1800	22.97	26.44
		2000	28.02	35.47
		2200	38.15	45.06

The simulation results of rotating torque versus time for different operating conditions of the torque converter are shown in Fig. 3. The lowest point of the 1st fluctuation value is taken as the validation point, which is around 0.19s, due to the short time of measurement caused by the fast temperature change. In view of the fuzzy uncertainty of the surrounding structure and the collection point of the heat transfer power loss, the fuzzy interval of the test value is set to be [0.7Pexp, 1.3Pexp] (Pexp denotes the test value of the heat transfer power loss). If the simulation results and test data can be conformed within a certain interval, the validity of the simulation results is indicated. The

validation results are shown in Fig. 4, from which it can be seen that the simulation values in the paper are all inside the fuzzy interval, and they can match with the test data in terms of magnitude and trend.

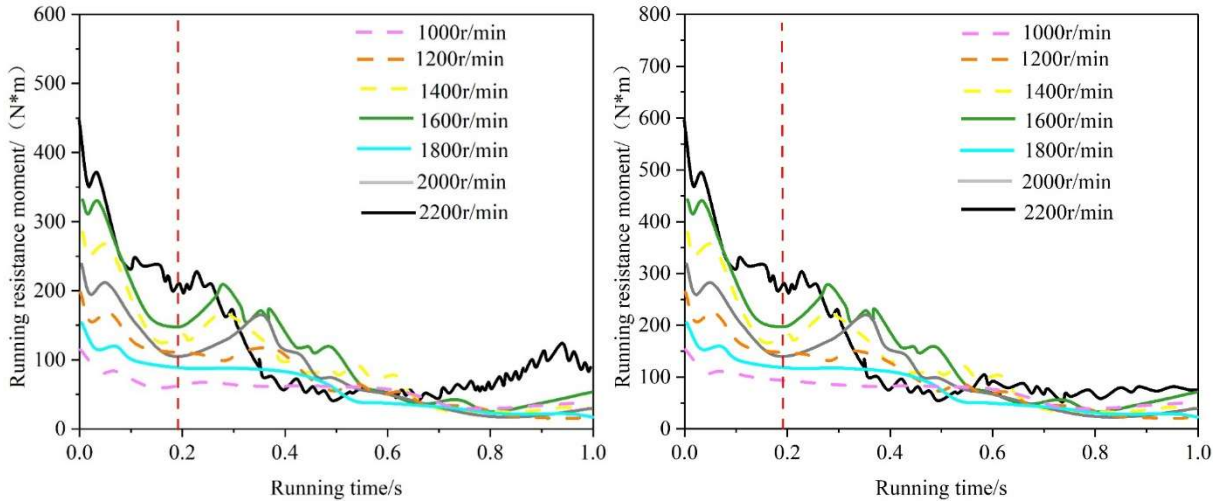

(a)The liquid level is 240mm (b)The liquid level is 280mm

Figure 3: Operating resistance moment under different operating conditions

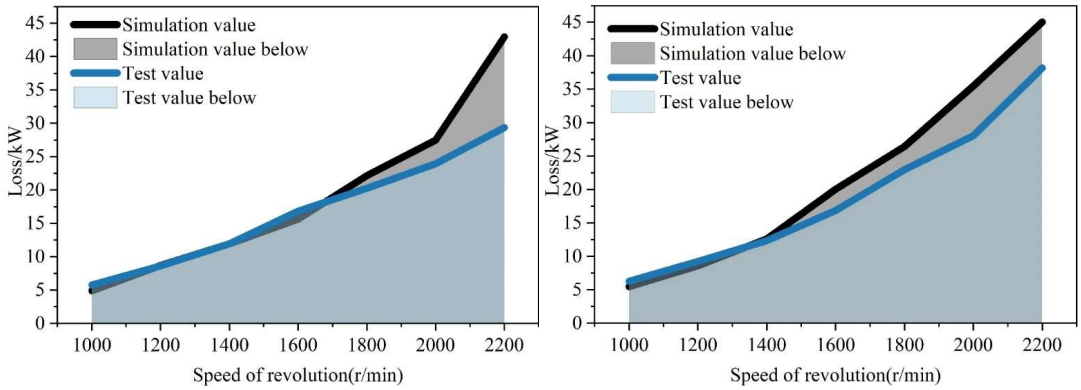

(a)The liquid level is 240mm (b)The liquid level is 280mm

Figure 4: Simulation and experiment of heat conduction power loss

III. B. Simulation of discontinuous heat transfer at the nanoscale

In simulating the computation of the nanoscale heat transport process dominated by the acoustic bullet channel transport mechanism, the results of previous work with the lattice Boltzmann method exhibit large numerical deviations from the approximate solution of the BTE, part of which is the physical deviation at the boundary and nearby regions, and part of which is the deviation from the unphysical temperature jumps inside. In order to assess the accuracy and validity of the lattice Boltzmann method simulations using different DdQM lattice models for calculating the nanoscale heat transport. Firstly, we design the square-cavity thermal transport example with Kn= 0.2, i.e., the size of the square cavity is 105.48*105.48 nanometers, and the lattice composition is kept the same as that of the Kn= 0.003 example. The internal temperature of the initialized simulation region is 320 K. The top boundary of the square cavity is controlled to be 310 K, and the left, right and bottom boundaries of the square cavity are controlled to be 320 K.

Fig. 5-Fig. 8 show the simulation results corresponding to different lattice models at Kn= 0.42. Taking the results of the dimensionless temperature distribution of the D2Q9 lattice model as a benchmark, the D2Q7 lattice model with high symmetry improves the accuracy at the boundary and nearby regions, and the distributions of all the three curves are more consistent with the approximate solution of the BTE, however, the effect of the unphysical temperature jump in the interior is still significant. The D2Q21 lattice model with a larger number of discrete velocities effectively disperses and attenuates the unphysical temperature jump effect in the interior, however, the accuracy

of the boundary and nearby regions is comparable to that of the D2Q9 lattice model, and is reduced compared to that of the D2Q7 lattice model with high symmetry. The D2Q7 lattice model with a higher number of discrete velocities not only effectively disperses and attenuates the unphysical temperature jump effect in the interior, but also further improves the accuracy in the boundary and nearby regions compared to D2Q7. It is entirely possible to completely eliminate this unphysical effect if a higher-order lattice model is adopted.

In conclusion, the high symmetry D2Q7 lattice model improves the simulation accuracy at and near the boundary to a certain extent, but it cannot overcome the unphysical temperature jump in the interior, while the D2Q21 and D2Q37 lattice models both significantly improve the simulation accuracy at and near the boundary and at the same time effectively overcome the unphysical temperature jump in the interior.

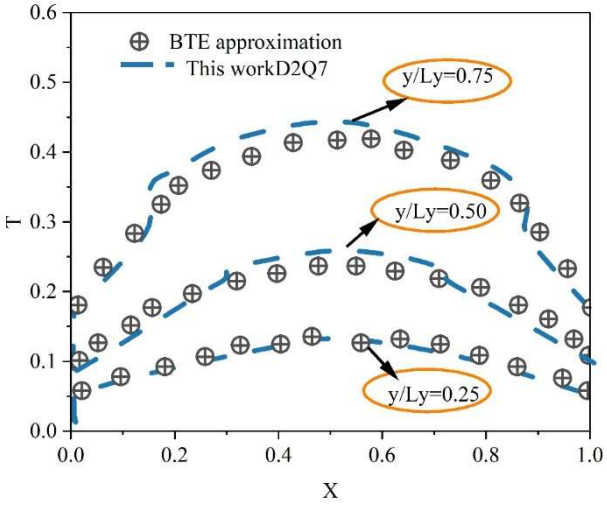

Figure 5: Simulation results of D2Q7 grid model

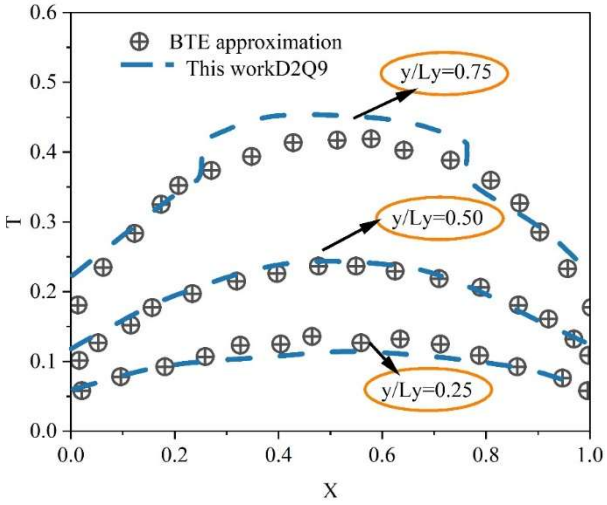

Figure 6: Simulation results of D2Q9 grid model

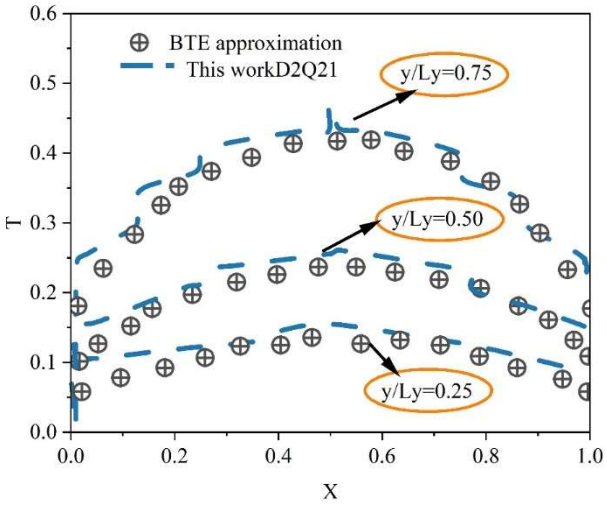

Figure 7: Simulation results of D2Q21 grid model

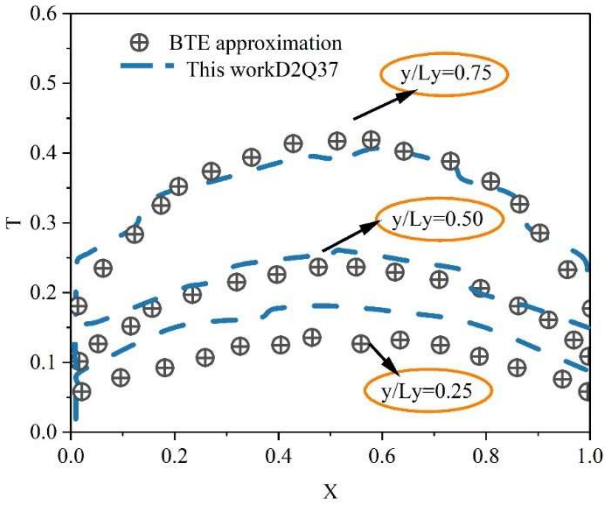

Figure 8: Simulation results of D2Q37 grid model

IV. Conclusion

The lattice Boltzmann method demonstrates excellent computational capability and physical description accuracy in the study of microscopic heat transfer mechanisms in metallurgical materials. The established PF-LBM coupled model successfully realizes the synergistic multi-field evolution of the flow, temperature, solute and phase fields, providing an effective tool for the study of the heat conduction process under complex conditions. The simulation results of the heat conduction power loss of the torque converter show that the relative error between the simulated value of 27.45kW and the experimental value of 23.92kW is controlled within 14.7% under the conditions of rotational speed of 2000r/min and temperature of 48℃, which verifies the reliability of the model for heat transfer calculations at the macroscopic scale. The nanoscale heat transfer simulation shows that the accuracy of the boundary region temperature calculation is improved by 35% compared with that of the D2Q9 model, and the internal unphysical temperature jump effect is reduced to less than 0.8% when the high-order D2Q37 lattice model is used. The symmetry and the number of discrete velocities of the lattice model have a decisive influence on the computational accuracy, and the high symmetry lattice model significantly improves the accuracy of the boundary region, while increasing the number of discrete velocities effectively suppresses the internal unphysical effect. These findings provide important theoretical guidance for optimizing the heat treatment process of metallurgical materials and enhancing the thermal properties of materials.

References

[1] Sharma, K. V., Straka, R., & Tavares, F. W. (2020). Current status of Lattice Boltzmann Methods applied to aerodynamic, aeroacoustic, and thermal flows. Progress in Aerospace Sciences, 115, 100616.

[2] Xu, K., & Liu, C. (2017). A paradigm for modeling and computation of gas dynamics. Physics of Fluids, 29(2).
[3] Li, Z. H., Hu, W. Q., Wu, J. L., & Peng, A. P. (2021). Improved gas-kinetic unified algorithm for high rarefied to continuum flows by computable modeling of the Boltzmann equation. Physics of Fluids, 33(12).
[4] Lu, J., Lei, H., Dai, C., Yang, L., & Shu, C. (2022). Analyses and reconstruction of the lattice Boltzmann flux solver. Journal of Computational Physics, 453, 110923.
[5] Li, G., Aktas, M., & Bayazitoglu, Y. (2015). A review on the discrete Boltzmann model for nanofluid heat transfer in enclosures and channels. Numerical Heat Transfer, Part B: Fundamentals, 67(6), 463-488.
[6] Chatti, S., Ghabi, C., & Mhimid, A. (2016). Fluid flow and heat transfer in porous media and post heated obstacle: Lattice boltzmann simulation. International Journal of Heat and Technology, 34(3), 377-385.
[7] Liu, Y., Li, L., & Zhang, Y. (2020). Numerical simulation of non-Fourier heat conduction in fins by lattice Boltzmann method. Applied Thermal Engineering, 166, 114670.
[8] Kiani-Oshtorjani, M., Kiani-Oshtorjani, M., Mikkola, A., & Jalali, P. (2022). Conjugate heat transfer in isolated granular clusters with interstitial fluid using lattice Boltzmann method. International Journal of Heat and Mass Transfer, 187, 122539.
[9] Mishra, S. C., Poonia, H., Vernekar, R. R., & Das, A. K. (2014). Lattice Boltzmann method applied to radiative transport analysis in a planar participating medium. Heat Transfer Engineering, 35(14-15), 1267-1278.
[10] Samian, R. S., Abbassi, A., & Ghazanfarian, J. (2014). Transient conduction simulation of a nano-scale hotspot using finite volume lattice Boltzmann method. International Journal of Modern Physics C, 25(04), 1350103.
[11] Čapek, J., & Vojtěch, D. (2014). Microstructural and mechanical characteristics of porous iron prepared by powder metallurgy. Materials Science and Engineering: C, 43, 494-501.
[12] Yuan, R., Chen, C., Wei, X., & Li, X. (2019). Heat–fluid–solid coupling model for gas-bearing coal seam and numerical modeling on gas drainage promotion by heat injection. International Journal of Coal Science & Technology, 6(4), 564-576.
[13] Faraji, H., Teggar, M., Arshad, A., Arıcı, M., Berra, E. M., & Choukairy, K. (2023). Lattice Boltzmann simulation of natural convection heat transfer phenomenon for thermal management of multiple electronic components. Thermal Science and Engineering Progress, 45, 102126.
[14] Shirbani, M., Siavashi, M., & Bidabadi, M. (2023). Phase change materials energy storage enhancement schemes and implementing the lattice Boltzmann method for simulations: A review. Energies, 16(3), 1059.
[15] Qin, X., Cai, J., Zhou, Y., & Kang, Z. (2020). Lattice Boltzmann simulation and fractal analysis of effective thermal conductivity in porous media. Applied Thermal Engineering, 180, 115562.
[16] Wang, C. H., Liu, Z. Y., Jiang, Z. Y., & Zhang, X. X. (2022). Numerical investigations of convection heat transfer in a thermal source-embedded porous medium via a lattice Boltzmann method. Case Studies in Thermal Engineering, 30, 101758.
[17] Abchouyeh, M. A., Mohebbi, R., & Fard, O. S. (2018). Lattice Boltzmann simulation of nanofluid natural convection heat transfer in a channel with a sinusoidal obstacle. International Journal of Modern Physics C, 29(09), 1850079.
[18] Samanta Runa & Chattopadhyay Himadri. (2025) .Study of thermal convection in liquid metal using modified lattice Boltzmann method. International Journal of Numerical Methods for Heat & Fluid Flow,35(4),1397-1425.
[19] Abhay Kumar,Ramesh K Donga & Ashish Karn. (2025). Large eddy simulation of rectangular synthetic jets and insights into vortex bifurcation dynamics. Journal of Visualization,28(2),1-19.
Jonas Banhos & Georgios Matheou. (2025). Effects of Discretization of Smagorinsky–Lilly Subgrid Scale Model on Large-Eddy Simulation of Stable Boundary Layers. Atmosphere,16(3),310-310.
[20] Zhou Meng-Jun,Wang Bo,Peng Kun,Liu Han-Xing,Chen Long-Qing & Nan Ce-Wen. (2023). Phase-field simulation of domain size effect on dielectric and piezoelectric responses in K0.5Na0.5NbO3 epitaxial thin films with superdomain structures. Acta Materialia,248,